

Synthesis of Mono- and Bisadducts of Thieno-*o*-quinodimethane with C₆₀ for Efficient Polymer Solar Cells

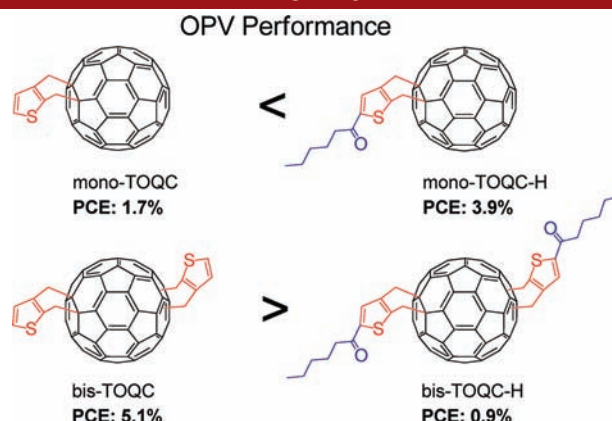
Congyun Zhang,[†] Shan Chen,[†] Zuo Xiao,^{*†} Qiqun Zuo,[‡] and Liming Ding^{*†}

National Center for Nanoscience and Technology, Beijing 100190, China, and Jiahong Optoelectronics, Suzhou 215151, China

opv.china@yahoo.com; xiaoz@nanoctr.cn

Received January 30, 2012

ABSTRACT



A series of mono- and bisadducts of thieno-*o*-quinodimethane with C₆₀ (TOQC) was efficiently prepared through the Diels–Alder reaction of pristine or solubilizing side-chain-substituted 2,3-bis(chloromethyl)thiophene with C₆₀. The pristine TOQC bisadduct (bis-TOQC) shows much higher performance than the side-chain-substituted TOQC bisadducts in polymer solar cells, while the situation is inverse for the TOQC monoadducts. The best power conversion efficiency of 5.1% was achieved from the bis-TOQC:P3HT solar cells under simulated AM1.5G irradiation (86 mW/cm²).

Organic photovoltaics (OPVs) employing electron-donating (p-type) and electron-accepting (n-type) organic semiconducting materials for cost-effective solar energy harvesting have become one of the most vibrant research areas.¹ For bulk heterojunction polymer solar cells, fullerenes and their derivatives have been recognized as the best acceptor materials due to their unique spherical structures, high electron affinity, and high electron mobility.² Recently, the development of fullerene bisadduct acceptors for high-performance polymer solar cells has received considerable attention due to the fact that the

open circuit voltage (V_{oc}) of the organic solar cells is proportional to the energy difference between the HOMO of the donor and the LUMO of the acceptor.³ Devices based on fullerene bisadducts with high LUMO levels should, in principle, afford high V_{oc} and high power conversion efficiency (PCE) if the short circuit current

(3) Rand, B. P.; Burk, D. P.; Forrest, S. R. *Phys. Rev. B* **2007**, *75*, 115327.

(4) (a) Lenes, M.; Wetzelaer, G.-J. A. H.; Kooistra, F. B.; Veenstra, S. C.; Hummelen, J. C.; Blom, P. W. M. *Adv. Mater.* **2008**, *20*, 2116. (b) He, Y. J.; Chen, H. Y.; Hou, J. H.; Li, Y. F. *J. Am. Chem. Soc.* **2010**, *132*, 5532. (c) Meng, X.; Zhang, W.; Tan, Z.; Du, C.; Li, C.; Bo, Z.; Li, Y.; Yang, X.; Zhen, M.; Jiang, F.; Zheng, J.; Wang, T.; Jiang, L.; Shu, C.; Wang, C. *Chem. Commun.* **2012**, *48*, 425. (d) Voroshazi, E.; Vasseur, K.; Aernouts, T.; Heremans, P.; Baumann, A.; Deibel, C.; Xue, X.; Herring, A. J.; Athans, A. J.; Lada, T. A.; Richtere, H.; Rand, B. P. *J. Mater. Chem.* **2011**, *21*, 17345. (e) Kim, K.-H.; Kang, H.; Nam, S. Y.; Jung, J.; Kim, P. S.; Cho, C.-H.; Lee, C.; Yoon, S. C.; Kim, B. J. *Chem. Mater.* **2011**, *23*, 5090. (f) Cheng, Y.-J.; Liao, M.-H.; Chang, C.-Y.; Kao, W.-S.; Wu, C.-E.; Hsu, C.-S. *Chem. Mater.* **2011**, *23*, 4056.

[†] National Center for Nanoscience and Technology.

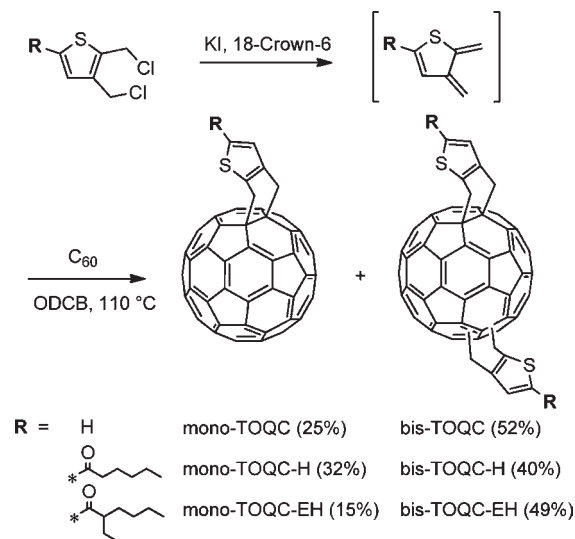
[‡] Jiahong Optoelectronics.

(1) Sun, S.-S.; Sariciftci, N. S. *Organic Photovoltaics: Mechanisms, Materials, and Devices*; Taylor and Francis: Boca Raton, FL, 2005.

(2) Hudhomme, P.; Cousseau, J. In *Fullerenes: Principles and Applications*; Langa, F., Nierengarten, J. F., Eds.; Royal Society of Chemistry: Cambridge, UK, 2007; Chapter 8.

(J_{sc}) and fill factor (FF) are fixed. Successful examples such as [6,6]-phenyl- C_{61} -butyric acid methyl ester bisadduct (bis- $PC_{61}BM$), indene- C_{60} bisadduct (ICBA), dihydronaphthyl- C_{60} bisadduct (NCBA), and di(4-methylphenyl)-methano- C_{60} bisadduct (DMPCBA) have been reported.⁴ With proper device optimization, up to ~50% increments in both V_{oc} and PCE have been achieved for these bisadduct-based solar cells in comparison to those standard $PC_{61}BM$ -based solar cells with poly(3-hexylthiophene) (P3HT) as the donor.

Scheme 1. Syntheses of TOQC Derivatives



Although remarkable progress has been made, the rules for designing efficient fullerene materials are obscure and rarely discussed. Meanwhile, there is plenty of room for developing new efficient acceptors through the chemical modification of fullerene. In this work, we synthesized a series of novel thiophene-containing fullerene derivatives, the thieno-*o*-quinodimethane- C_{60} (TOQC) mono- and bisadducts, through the Diels–Alder reaction and investigated the synergistic influence of the LUMO energy levels and the solubilizing side chains to the final photovoltaic performance of the fullerene acceptors. Our results indicate that not all bisadducts of fullerene with high LUMO levels are efficient acceptors for OPVs. The acceptor based on pristine TOQC bisadduct (no side chains) gave the highest performance (PCE = 5.1%), while the side-chain-substituted TOQC bisadducts show much lower efficiency due to low J_{sc} and FF. On the contrary, the side-chain-substituted TOQC monoadducts show much higher PCE than the pristine one due to their improved solubility.

The design for TOQC is based on the following considerations: first, the introduction of a thiophene moiety to fullerene can help to improve the miscibility between donor and acceptor;⁵ second, the 5-position of the thiophene ring is easy to functionalize with solubilizing chains. TOQC

derivatives were prepared through the [2 + 4] cycloaddition reaction of C_{60} and the in situ generated thieno-*o*-quinodimethane dienes by a published method (Scheme 1).⁶ Pristine ($R = H$) and substituted ($R =$ hexanoyl or 2-ethylhexanoyl) 2,3-bis(chloromethyl)thiophene were used as the precursors for thieno-*o*-quinodimethane and were prepared according to the literature.⁷ To obtain both mono- and bisadducts of TOQC, we employed 2 equiv of precursor for all reactions. In comparison to *o*-quinodimethane, thieno-*o*-quinodimethane is more reactive, and all reactions were completed within 30 min. The yields for the mono- and bisadducts of TOQC are 15–32 and 40–52%, respectively.

The NMR spectra indicate that the monoadducts of TOQC are isomerically pure compounds with C_s symmetry while the bisadducts of TOQC are isomers as expected (Figures S1–S12 in Supporting Information). The MALDI-TOF mass spectra show the expected molecular ion peaks for all compounds. The UV–vis spectra of the pristine mono-TOQC, bis-TOQC, and the reference $PC_{61}BM$ are shown in Figure 1. Both mono-TOQC and $PC_{61}BM$ show the characteristic absorption of the fullerene 1,2-adduct at 433 and 428 nm, respectively, while bis-TOQC shows enhanced absorption in the 440–510 nm region. The side-chain-substituted derivatives, mono-TOQC-H, bis-TOQC-H, mono-TOQC-EH, and bis-TOQC-EH, show similar absorption spectra as their pristine analogues (Figure S13). The side-chain-substituted TOQCs are highly soluble in common organic solvents. For example, their solubilities are over 3 wt % in chloroform and over 6 wt % in *o*-dichlorobenzene (ODCB). The solubility is also good for the pristine bis-TOQC, about 1.5 wt % in ODCB but is quite low for the pristine mono-TOQC, only 0.4 wt % in ODCB.

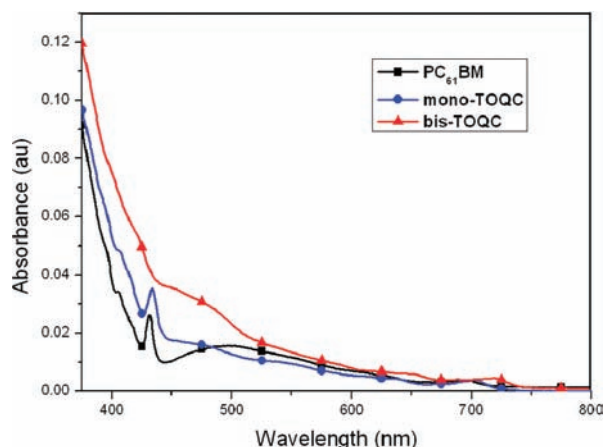


Figure 1. UV–vis absorption spectra for mono-TOQC, bis-TOQC, and $PC_{61}BM$ in chloroform (10^{-5} mol/L).

(5) Popescu, L. M.; van't Hof, P.; Sieval, A. B.; Jonkman, H. T.; Hummelen, J. C. *Appl. Phys. Lett.* **2006**, *89*, 213507.

(6) (a) Belik, P.; Gügel, A.; Spickermann, J.; Müllen, K. *Angew. Chem., Int. Ed. Engl.* **1993**, *32*, 78. (b) Fernandez-Paniagua, U. M.; Illescas, B. M.; Martin, N.; Seoane, C. *J. Chem. Soc., Perkin Trans. 1*, 1077.

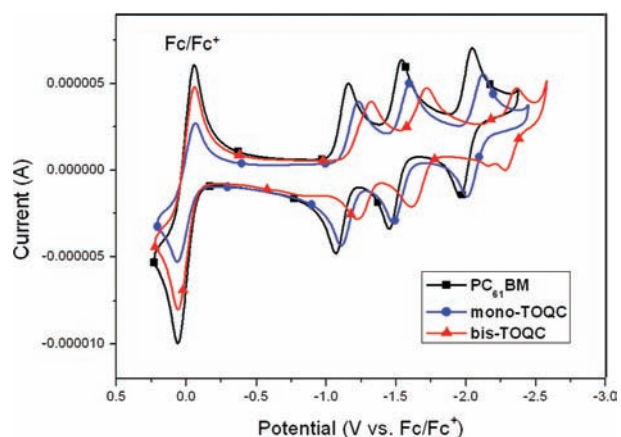


Figure 2. Cyclic voltammograms of mono-TOQC, bis-TOQC, and PC₆₁BM (0.001 mol/L) in ODCB/CH₃CN (5:1) solution with TBAPF₆ (0.1 mol/L) at a scan rate of 100 mV/s.

The electrochemical properties of TOQC derivatives were evaluated by cyclic voltammetry (CV) methods. Figure 2 shows a representative comparison of the CV for mono-TOQC, bis-TOQC, and PC₆₁BM. All reduction potentials of mono-TOQC and bis-TOQC shift negatively compared to that of PC₆₁BM. Similar results were also found for side-chain-substituted TOQC derivatives (Figure S14). The half-wave reduction potentials and the estimated LUMO levels of the fullerene acceptors are listed in Table 1. The LUMO levels of all TOQC monoadducts are slightly higher than that of PC₆₁BM, whereas the LUMO levels of the TOQC bisadducts are ~0.1 eV higher than that of the monoadducts. The elevation of the LUMO energy levels along with the number of addition is a common feature for fullerene derivatives reflecting the reduction in electron affinity on the fullerene sphere. The side chains, on the other hand, have no dramatic effect on the LUMO energy levels of the TOQCs. The higher LUMO levels of the TOQC bisadducts are favorable for OPV applications because of the potential for high V_{oc} .

Table 1. Half-Wave Reduction Potentials^a and LUMO Energy Levels^b of PC₆₁BM and TOQC Derivatives

fullerenes	E_1 (V)	E_2 (V)	E_3 (V)	LUMO (eV)
PC ₆₁ BM	-1.11	-1.50	-2.00	-3.69
mono-TOQC	-1.17	-1.54	-2.06	-3.63
mono-TOQC-H	-1.12	-1.55	-2.02	-3.68
mono-TOQC-EH	-1.15	-1.56	-2.05	-3.65
bis-TOQC	-1.27	-1.66	-2.31	-3.53
bis-TOQC-H	-1.27	-1.66	-2.39	-3.53
bis-TOQC-EH	-1.23	-1.62	-2.31	-3.57

^a Potential values are versus Fc/Fc⁺ reference electrode. ^b LUMO energy levels were estimated using the following equation: LUMO level = $-(E_1 + 4.8)$ eV.⁸

The thermal properties of TOQCs were evaluated by thermogravimetric analysis (TGA) and differential

scanning calorimetry (DSC). The decomposition temperatures (5% weight loss) for TOQC derivatives are generally over 200 °C, indicating that they are sufficiently thermally stable for OPV applications (Figure S15). The DSC results show no obvious phase transition peaks for TOQCs, suggesting their amorphous feature (Figure S16).⁸

We fabricated the bulk heterojunction solar cells with a typical structure ITO/PEDOT:PSS/fullerene:P3HT/Ca/Al. The concentration for all blend solutions in ODCB was optimized to be 24 mg/mL except mono-TOQC:P3HT blend, which is 10 mg/mL due to the low solubility of mono-TOQC. The donor–acceptor ratio and the annealing temperature for the devices were optimized to be 1:0.6 and 150 °C, respectively (Figures S17 and S18). The OPV performances of all fullerene materials under AM1.5G, 86 mW/cm² illumination are listed in Table 2. Compared with the reference PC₆₁BM solar cell, slightly higher V_{oc} values (0.63–0.64 V) were obtained for TOQC monoadduct devices. This corresponds with the slightly higher LUMO levels of the TOQC monoadducts. The PCE for the solar cells of the side-chain-substituted monoadducts, mono-TOQC-H and mono-TOQC-EH, are 3.9 and 3.4%, respectively, which are comparable to that of the PC₆₁BM cell, 3.6%. The PCE and J_{sc} of the mono-TOQC solar cell, on the other hand, are only half of that of the mono-TOQC-H and mono-TOQC-EH cells. The low J_{sc} is caused by the low concentration of the blend solution of mono-TOQC, which leads to a thin active layer. The thickness of the active layer is ~60 nm for the mono-TOQC device, while it is ~110 nm for mono-TOQC-H and mono-TOQC-EH devices. The champion cell is based on the blend of P3HT and the pristine fullerene bisadduct, bis-TOQC. This device afforded a high PCE of 5.1%, which is 42% higher than that of the PC₆₁BM device. Obviously, the PCE improvement results from high V_{oc} (0.86 V), which is 39% higher than that of the PC₆₁BM device. The higher V_{oc} benefits from the higher LUMO level of the bis-TOQC molecules. In sharp contrast to bis-TOQC, the OPV performance of the side-chain-substituted bisadducts, bis-TOQC-H and bis-TOQC-EH, is very low

Table 2. Performance of the Solar Cells Based on P3HT and Different Acceptors (1:0.6, w/w)^a

acceptors	V_{oc} (V)	J_{sc} (mA/cm ²)	FF	PCE (%)
PC ₆₁ BM	0.62	8.2	0.61	3.6
mono-TOQC ^b	0.63	4.1	0.57	1.7
mono-TOQC-H	0.63	8.7	0.61	3.9
mono-TOQC-EH	0.64	8.3	0.55	3.4
bis-TOQC	0.86	7.7	0.66	5.1
bis-TOQC-H	0.67	2.8	0.39	0.9
bis-TOQC-EH	0.73	3.4	0.38	1.1

^a Blend concentration: 24 mg/mL in ODCB; annealing temperature = 150 °C. ^b Blend concentration: 10 mg/mL in ODCB.

(7) (a) Hammer, K.; Benneche, T.; Hope, H.; Undheim, K. *Acta Chem. Scand.* **1997**, *51*, 392. (b) Hou, J. H.; Chen, H. Y.; Zhang, S. Q.; Chen, R. I.; Yang, Y.; Wu, Y.; Li, G. *J. Am. Chem. Soc.* **2009**, *131*, 15586.

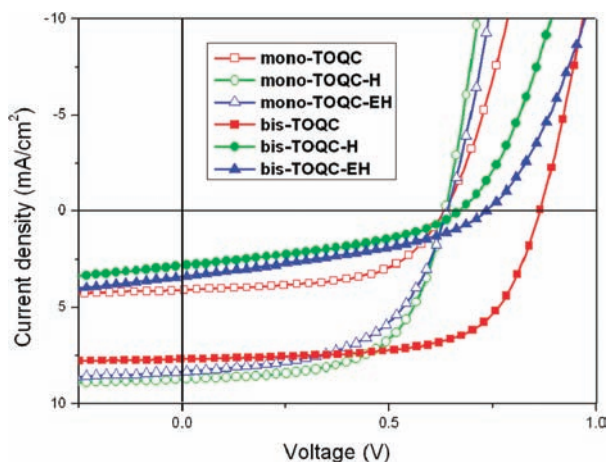


Figure 3. J – V curves for TOQC mono- and bisadducts.

(Figure 3). Although good V_{oc} values of 0.67 and 0.73 V were obtained for bis-TOQC-H and bis-TOQC-EH devices, respectively, the J_{sc} and FF are much lower than that of other fullerene devices, suggesting poor electron transport properties of bis-TOQC-H and bis-TOQC-EH. MacKenzie et al. theoretically predicted that the carrier mobility of the fullerene monoadduct significantly decreases as the solubilizing group size increases because the bulky side chain can inhibit the stacking of fullerene, blocking electron transport.⁹ For fullerene bisadducts, the electron transport might be more sensitive to the side chains because more side chains block fullerene stacking.

(8) Matsuo, Y.; Iwashita, A.; Abe, Y.; Li, C. Z.; Matsuo, K.; Hashiguchi, M.; Nakamura, E. *J. Am. Chem. Soc.* **2008**, *130*, 15429.

(9) MacKenzie, R. C.; Frost, I. J. M.; Nelson, J. *J. Chem. Phys.* **2010**, *132*, 064904.

In the cases of bis-TOQC-H and bis-TOQC-EH, this blocking effect is remarkable; for bis-TOQC, high J_{sc} and FF can be obtained because no side chains interfere with fullerene stacking.

In conclusion, we have achieved up to 5.1% power conversion efficiency from polymer solar cells based on a series of newly developed thieno-*o*-quinodimethane- C_{60} . The effect of solubilizing side chains on the OPV performance of the fullerene monoadducts and bisadducts is dramatically different: for monoadducts, the side chains can effectively improve the solubility of the materials and help to improve the performance; for bisadducts, the side chains significantly lower the device performance because the side chains interfere with fullerene stacking, leading to poor electron transport in the fullerene domain. These results may shed light on rational design of efficient fullerene acceptors for OPV applications. Further work on balancing solubility, LUMO levels, and electron transport of fullerene acceptors is ongoing.

Acknowledgment. This work was supported by the “100 Talents Program” of the Chinese Academy of Sciences and National Natural Science Foundation of China (21102028). Funding from Suzhou Jiahong Optoelectronics and the Ministry of Science and Technology of China is greatly appreciated. We also thank Professor Jinsong Zhu of National Center for Nanoscience and Technology for kindly gifting a MBRAUN glovebox, and Professor Zhong Zhang of National Center for Nanoscience and Technology for providing laboratory space.

Supporting Information Available. Experimental procedures and spectral data for all new compounds. This material is available free of charge via the Internet at <http://pubs.acs.org>.

The authors declare no competing financial interest.